J|A|C|S
ARTICLES
Published on Web 07/04/2006

Toward the Control of the Magnetic Anisotropy of Fe^{II} Cubes: A DFT Study

Jordi Ribas-Arino,*,† Tunna Baruah,‡ and Mark R. Pederson*,§

Contribution from the Departament de Química Física, Facultat de Química i Centre Especial de Recerca en Química Teórica, Parc Científic, Universitat de Barcelona, Av. Diagonal 647, Barcelona 08028, Spain, Department of Physics, University of Texas at El Paso, El Paso, Texas, 79968, and Center for Computational Materials Science, Code 6392, Naval Research Laboratory, Washington, D.C. 20375-5000

Received March 16, 2006; E-mail: jribasjr@yahoo.es; pederson@dave.nrl.navy.mil

Abstract: We present the results of our all-electron density-functional calculations on the magnetic anisotropy of the $[Fe_4(sap)_4(MeOH)_4]$ and $[Fe_4(sae)_4(MeOH)_4]$ polynuclear complexes. Our calculations, which predict that only the second complex is a single-molecule magnet (with a magnetic anisotropy energy barrier of 5.6 K), are in qualitative agreement with the experimental data. The analysis of the projected anisotropies of each Fe^{II} ion, together with a study of the variation of the *D* value as a function of several geometrical parameters, allows us to qualitatively understand the different magnetic behaviors of both complexes. In addition to this, we also present a simple rule based on the analysis of the molecular orbitals of the system that allows us to predict how to enhance (by a factor of 6, approximately) the magnetic anisotropy barrier of these systems. Specifically, we will show that, for high-spin Fe^{II} ions, the local easy axis of magnetization is perpendicular to the plane defined by the Fe^{II}-d orbital which is doubly occupied. If similar rules were found for other metal ions, rational synthetic strategies to control magnetic anisotropy could be established.

Introduction

High-spin molecules having an energy barrier that prevents easy reversal of the magnetic moment are being extensively studied due to their potential technological applications to new data storage systems and to quantum computing.[1] This kind of molecules show slow magnetic relaxation with respect to spin flipping along the magnetic anisotropy axis. At very low temperatures, the spin does not have enough thermal energy in order to overcome the energy barrier, but it can flip by means of quantum processes. Because of this superparamagnetic behavior, these molecules are called single-molecule magnets (SMMs).[2] The first polynuclear complex which was reported to behave as an SMM was the $Mn_{12}Ac$ complex[3]. Since then, other SMMs containing manganese[4] (including several analogues of the $Mn_{12}Ac$ polynuclear complex), iron,[5] nickel,[6] and cobalt[7] ions have been reported.

Recently, a new series of Fe^{II}-based polynuclear complexes showing the SMM behavior have been prepared.[8] These new SMMs have tetranuclear cubane core structures, in which four Fe^{II} ions are linked together by μ_3-alkoxo groups, thus yielding an approximately cubic array of alternating iron and oxygen atoms. In these polynuclear complexes, the six coordination sites of each Fe^{II} are occupied by five oxygen atoms and one nitrogen atom from a chelating Schiff base ligand and methanol molecules. The chelating Schiff base ligands are derivatives of the sae^{2-} ligand (Figure 1), which are prepared by condensation of salicylaldehyde derivatives with aminoethyl alcohol. One relevant fact is that when the sae^{2-} derivatives are replaced with sap^{2-}derivatives (the sap^{2-} ligand derivatives are prepared by condensation of salicylaldehyde derivatives with aminopropyl alcohol), the resultant complexes no longer behave as SMMs. The only difference between the sap^{2-} ligands and the sae^{2-} ligands is (Figure 1) that the former ones can form six-membered chelate rings with the Fe^{II} ions, whereas the latter ones can only form five-membered chelate rings because they have one less $-CH_2-$ unit. This causes different steric strains and enhances the Jahn−Teller distortions at Fe^{II} centers, which results in a different magnetic behavior of the whole polynuclear complex. This finding is remarkable, since it shows that the magnetic anisotropy of polynuclear complexes can be structurally controlled.

Here we present an all-electron density-functional calculation on the second-order magnetic anisotropy of one of the com-

† Universitat de Barcelona.
‡ University of Texas at El Paso.
§ Naval Research Laboratory.

(1) (a) Gatteschi, D.; Caneschi, A.; Pardi, L.; Sessoli, R. *Science* **1994**, *265*, 1054. (b) Müller, A.; Peters, F.; Pope, M. T.; Gatteschi, D. *Chem. Rev.* **1998**, *98*, 239. (c) Wernsdorfer, W.; Sessoli, R. *Science* **1999**, *284*, 133. (d) Leuenberger, M. N.; Loss, D. *Nature* **2001**, *410*, 789. (e) Hill, S.; Edward, R. S.; Aliaga-Alcalde, N.; Christou, G. *Science* **2003**, *302*, 1015.
(2) (a) Friedman, J. R.; Sarachik, M. P.; Tejada, J.; Ziolo, R. *Phys. Rev. Lett.* **1996**, *76* (20), 3830. (b) Thomas, L.; Lionti, L.; Ballou, R.; Gatteschi, D.; Sessoli, R.; Barbara, B. *Nature* **1996**, *383*, 145. (c) Tejada, J.; Ziolo, R. F.; Zhang, X. X. *Chem. Mater.* **1996**, *8*, 41784. (d) Aubin, S. M.; Gilley, N. R.; Pardi, L.; Krzystek, J.; Wemple, M. W.; Brunel, L. C.; Marple, M. B.; Christou, G.; Hendrickson, D. N. *J. Am. Chem. Soc.* **1998**, *120*, 4991. (e) Ruiz, D.; Sun, Z.; Albela, B.; Folting, K.; Christou, G.; Hendrickson, D. N. *Angew. Chem., Int. Ed.* **1998**, 300.
(3) (a) Lis, T. *Acta Crystallogr., Sect. B* **1980**, *36*, 2042. (b) Sessoli, R.; Gatteschi, D.; Caneschi, A.; Novak, M. A. *Nature* **1993**, *115*, 1804. (c) Sessoli, R.; Tsai, H.-L.; Schake, A. R.; Wang, S.; Vincent, J. B.; Folting, K.; Gatteschi, D.; Christou, G.; Hendrickson, D. N. *J. Am. Chem. Soc.* **1993**, *115*, 1804.

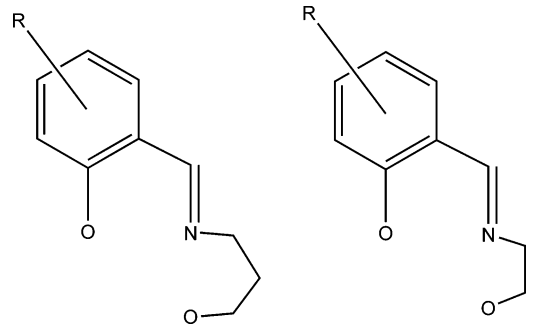

Figure 1. Structure of the sap^{2-} ligand derivatives (left) and structure of the sae^{2-} ligand derivatives (right).

plexes of the series prepared with the sap^{2-} ligand derivatives and of one of the complexes of the series prepared with the sae^{2-} ligand derivatives. To be specific, we present the results for the $[Fe_4(sap)_4(MeOH)_4]$ compound (Figure 2) (complex **1**) and for the $[Fe_4(sae)_4(MeOH)_4]$ compound (Figure 3) (complex **2**). We also present an analysis of the structural and electronic factors responsible for the change in the magnetic anisotropy of both complexes. Finally, based on the results of this analysis we propose a means for increasing, by a factor of 6, the magnetic anisotropy energy (MAE) barrier (which is the energy barrier that has to be overcome in the reversal of the magnetic moment of the molecule) of this kind of Fe^{II}-cubane-based SMMs. Specifically, we will show how the π-back-donation of the Fe^{II} ions to the ligands allows one to easily control the sign and magnitude of the *D* (zero-field splitting parameter) value and, consequently, the height of the MAE barrier. This is the first

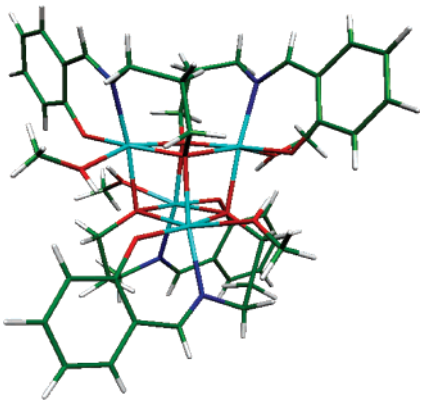

Figure 2. Structure of the $[Fe_4(sap)_4(MeOH)_4]$ compound, which has an S_4 symmetry. The chelating ligand in this compound is the simplest one of the series of the sap ligand derivatives; that is to say, it has no substituents attached to the benzenic ring.

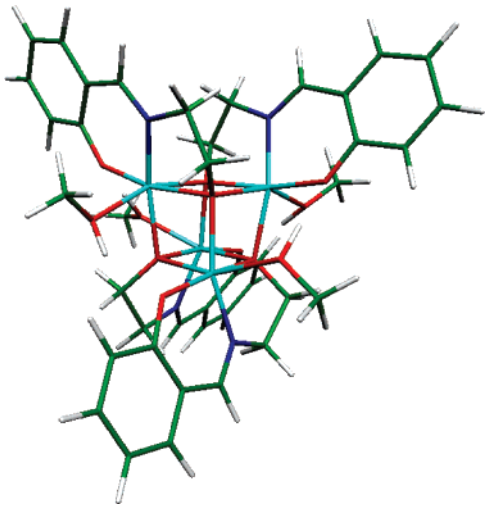

Figure 3. Structure of the $[Fe_4(sae)_4(MeOH)_4]$ compound, which has no symmetry. The chelating ligand in this compound is the simplest one of the series of the sae ligand derivatives; that is to say, it has no substituents attached to the benzenic ring.

time that DFT calculations of the magnetic anisotropy have aided in identifying a qualitative and simple rule (based on the electronic properties of the ligands) to control and enhance the magnetic anisotropy of a specific system. Moreover, this simple and new rule can be applied not only to the specific systems studied in this article but also to other Fe^{II}-based complexes. Therefore, our DFT calculations should facilitate the rational synthesis of a new whole family of Fe^{II}-based SMMs and, eventually, the preparation of technologically useful SMMs. Taking into account that most of the SMMs reported so far have been found by serendipity, it is clear that all these results will be very useful in the field of nanomagnetism.

Theory

The MAE barrier is related to the zero-field splitting of the spin states due to spin−orbit coupling. The spin−orbit interaction is given by

$$U = -\frac{1}{2c^2} S \cdot p \times \nabla\Phi(r) \cong \frac{1}{2c^2} L \cdot S \frac{1}{r} \frac{d\phi(r)}{dr} = \lambda L \cdot S \quad (1)$$

We use the first form given in the above equation. The second and third forms are approximations. The second form is correct

(4) (a) Caneschi, A.; Gatteschi, D.; Sessoli, R.; Barra, A. L.; Brunel, L. C.; Guillot, M. J. *J. Am. Chem. Soc.* **1991**, *113*, 5873. (b) Friedman, J. R.; Sarachik, M. P.; Tejada, J.; Maciejewski, J.; Ziolo, R. *J. Appl. Phys.* **1996**, *79*, 6031. (c) Eppley, H. J.; Tsai, H.-L.; De Vries, N.; Folting, K.; Christou, G.; Hendrickson, D. N. *J. Am. Chem. Soc.* **1995**, *117*, 301. (d) Boskovic, C.; Pink, M.; Huffman, J. C.; Hendrickson, D. N.; Christou, G. *J. Am. Chem. Soc.* **2001**, *123*, 9914. (e) Soler, M.; Wernsdorfer, W.; Abboud, K. A.; Huffman, J. C.; Davidson, E. R.; Hendrickson, D. N.; Christou, G. *J. Am. Chem. Soc.* **2003**, *125*, 3576. (f) Boskovic, C.; Brechin, E. K.; Streib, W. E.; Folting, K.; Bollinger, J. C.; Hendrickson, D. N.; Christou, G. *J. Am. Chem. Soc.* **2003**, *124*, 3725. (g) Brechim, E. K.; Boskovic, C.; Wernsdorfer, W.; Yoo, J.; Yamaguchi, A.; Sanudo, E. C.; Concolino, T. R.; Rheingold, A. L.; Ishimoto, H.; Hendrickson, D. N.; Christou, G. *J. Am. Chem. Soc.* **2002**, *124*, 9710. (h) Wernsdorfer, W.; Aliaga-Alcalde, N.; Hendrickson, D. N.; Christou, G. *Nature* **2002**, *416*, 406. (i) Aromi, G.; Bhaduri, S.; Artus, P.; Folting, K.; Christou, G. *Inorg. Chem.* **2002**, *41*, 805. (j) Price, J. P.; Batten, S. R.; Moubaraki, B.; Murray, K. S. *Chemm. Commun.* **2002**, 762. (k) Brockman, J. T.; Huffman, J. C.; Christou, G. *Angew. Chem., Int. Ed.* **2002**, *41*, 2506. (l) Soler, M.; Artus, P.; Folting, K.; Huffman, J. C.; Hendrickson, D. N.; Christou, G. *Inorg. Chem.* **2001**, *40*, 4902. (m) Aliaga-Alcalde, N.; Folting, K.; Hendrickson, D. N.; Christou, G. *Polyhedron* **2001**, *20*, 1273. (n) Andres, H.; Basler, R.; Gudel, H.-U.; Aromi, G.; Christou, G.; Buttner, H.; Ruffle, B. *J. Am. Chem. Soc.* **2000**, *122*, 12469. (o) Artus, P.; Boskovic, C.; Yoo, J.; Streib, W. E.; Brunel, L.-C.; Hendrickson, D. N.; Christou, G. *Inorg. Chem.* **2001**, *40*, 4199. (p) Soler, M.; Rumberger, E.; Folting, K.; Hendrickson, D. N.; Christou, G. J. *Polyhedron* **2001**, *20*, 1365. (q) Aubin, S. M. J.; Sun, Z.; Pardi, L.; Krzystek, J.; Folting, K.; Brunel, L.-C.; Rheingold, A. L.; Christou, G.; Hendrickson, D. N. *Inorg. Chem.* **1999**, *38*, 5329. (r) Aubin, S. M. J.; Wemple, M. W.; Adams, D. M.; Tsai, H.-L.; Christou, G.; Hendrickson, D. N. *J. Am. Chem. Soc.* **1996**, *118*, 7746. (s) Gatteschi, D.; Sessoli, R.; Cornia, A. *Chem. Commun.* **2000**, 725. (t) Barra, A. L.; Debrunner, P.; Gatteschi, D.; Schulz, C. E.; Sessoli, R. *Europhys. Lett.* **1996**, *35*, 133.
(5) (a) Sangregorio, C.; Ohm, T.; Paulsen, C.; Sessoli, R.; Gatteschi, D. *Phys. Rev. Lett.* **1997**, *78*, 4645. (b) Barra, A. L.; Caneschi, A.; Cornia, A.; Fabrizi de Biani, F.; Gatteschi, D.; Sangregorio, C.; Sessoli, R.; Sorace, L. *J. Am. Chem. Soc.* **1999**, *121*, 5302. (c) Cornia, A.; Fabretti, A. C.; Garrisi, P.; Mortalò, C.; Bonacchi, D.; Gatteschi, D.; Sessoli, R.; Sorace, L.; Wernsdorfer, W.; Barra, A.-L. *Angew. Chem., Int. Ed.* **2004**, *43*, 1136.
(6) Cadiou, C.; Murrie, M.; Paulsen, C.; Villar, V.; Wernsdorfer, W.; Winpenny, R. E. P. *Chem. Commun.* **2001**, 2666.
(7) Yang, E.-C.; Hendrickson, D. N.; Wernsdorfer, W.; Nakano, M.; Zakharov, L. N.; Sommer, R. D.; Rheingold, A. L.; Ledezma-Gairaud, M.; Christou, G. *J. Appl. Phys.* **2002**, *91*, 7382.
(8) (a) Oshio, H.; Hoshino, N.; Ito, T.; Nakano, M. *J. Am. Chem. Soc.* **2004**, *126*, 8805. (b) Oshio, H.; Hoshino, N.; Ito, T. *J. Am. Chem. Soc.* **2000**, *122*, 12602.

in the limit of spherical symmetry. The third form also requires spherical symmetry but further assumes that there is only one radial matrix element, λ, of interest. For more details, we refer the interested reader to ref 9. It can be shown[9] that, up to second-order perturbation theory, the change in the energy of a system due to spin−orbit coupling at zero applied magnetic field can be expressed as

$$\Delta_2 = \sum_{\sigma\sigma'} \sum_{ij} M_{ij}^{\sigma\sigma'} S_i^{\sigma\sigma'} S_j^{\sigma\sigma'} \tag{2}$$

where

$$S_i^{\sigma\sigma'} = \langle \chi^{\sigma} | S_i | \chi^{\sigma'} \rangle \tag{3}$$

and

$$M_{ij}^{\sigma\sigma'} = -\sum_{kl} \frac{\langle \phi_{l\sigma} | V_i | \phi_{k\sigma'} \rangle \langle \phi_{k\sigma'} | V_j | \phi_{l\sigma} \rangle}{\epsilon_{i\sigma} - \epsilon_{k\sigma'}} \tag{4}$$

In eq 3, χ^{σ} and $\chi^{\sigma'}$ are any set of spinors, and the S_i are the spin operators. In eq 4, $\phi_{l\sigma}$ and $\phi_{k\sigma'}$ are, respectively, the occupied and unoccupied states, and the ϵ's are the corresponding Kohn−Sham energies. The V_i matrix elements are related to the derivative of the Coulomb potential as defined in eq 7 of ref 9. The matrix elements $S_i^{\sigma\sigma'}$ explicitly depend on the orientation of the axis of quantization, and that is what gives rise to the anisotropy energy. It can be shown that the above expression for the second-order shift in the energy of the system in the absence of a magnetic field can be rewritten as

$$\Delta_2 = \sum_{xy} \gamma_{xy} \langle S_x \rangle \langle S_y \rangle \tag{5}$$

By diagonalizing the anisotropy tensor (γ), the principal axes and eigenvalues (γ_x,γ_y,γ_z) are determined. Once the anisotropy tensor has been diagonalized, the second-order energy can be rewritten, in principle-axes space, in terms of the eigenvalues according to

$$\Delta_2 = \frac{1}{3}(\gamma_x + \gamma_y + \gamma_z) S(S+1) + \frac{1}{3}\left[\gamma_z - \frac{1}{2}(\gamma_x + \gamma_y)\right][3S_z^2 - S(S+1)] + \frac{1}{2}(\gamma_x - \gamma_y)(S_x^2 - S_y^2) \tag{6}$$

In the above equation, the operators S_x, S_y, and S_z are rotated relative to the coordinate system in eqs 1−5 according to the eigenvectors of the anisotropy tensor. The anisotropy Hamiltonian splits the $(2S + 1)$ spin states, and ignoring the isotropic $S(S + 1)$ terms, it can be expressed as

$$H = DS_z^2 + E(S_x^2 - S_y^2) \tag{7}$$

Therefore, the D and E values can be directly obtained from the γ_{xx}, γ_{yy}, and γ_{zz} values. The eigenvalues of the anisotropy Hamiltonian (eq 7) are the energies of the total azimuthal spin levels (M_S). The difference in energy between the highest total azimuthal spin level and the lowest total azimuthal spin level yields the MAE barrier in easy-axis systems. It may be mentioned that this MAE barrier is a classical barrier in the sense that it does not take into consideration the quantum tunneling effects.

The theoretical method described here has been reported to be a reliable one in order to predict magnetic anisotropy parameters of SMMs.[10] Finally, the atom-projected anisotropies on each iron ion have been calculated using the method described in ref 11.

Table 1. Maximum and Minimum Exponents of the Bare Gaussians, the Number of Bare Gaussians, and the Number of Contracted Gaussians for Each Angular Momentum for Different Atoms Used in the Calculation of the Fe^{II}-Based Molecular Complexes[a]

atom	α_{max}	α_{min}	N_{bare}	s	p	d
H	77.84	0.0745	6	2	1	0
C	2.2×10^4	0.0772	12	5	4	1
N	5.1×10^4	0.0941	13	5	4	1
O	6.1×10^4	0.1049	13	5	4	1
Fe	3.8×10^6	0.0452	20	6	4	4

[a] Basis sets can be furnished upon request to first author.

Computational Details

The density-functional theory[12] (DFT) calculations discussed herein were performed with the all-electron Gaussian-orbital-based NRLMOL[13] program. All calculations employed the Perdew−Burke−Ernzerhof[14] (PBE) generalized-gradient approximation for the density functional. The exponents for the single Gaussians of the basis set have been fully optimized for DFT calculations.[15] The NRLMOL code employs a variational mesh for numerically precise integration and an analytic solution of Poisson's equation.

The basis set employed consisted of a total of 1848 basis functions for the $[Fe_4(sap)_4(MeOH)_4]$ (complex **1**) calculation and of a total of 1716 basis functions for the $[Fe_4(sae)_4(MeOH)_4]$ (complex **2**) calculation. Basis set details are summarized in Table 1.

In the present work, a large energy window from −39.7 eV below the Fermi energy to 10.6 eV above the Fermi energy (for complex **1**) and from −39.8 to 10.5 eV (for complex **2**) was used to calculate the matrix elements of eq 4.

Results

The optimized structures of complex **1** and complex **2** are depicted in Figure 2 and Figure 3, respectively. The Fe^{II} coordination bond lengths of both complexes are given in Table 2. With reference to the spin topology of the electronic state of both complexes, the calculations have been performed for the $S = 8$ state (the magnetic exchange interaction between all the Fe^{II} ions is ferromagnetic), which is the ground electronic state, according to the experimental data.[8] The calculated local moment, determined by integrating the spin density within a sphere of radius 2.19 bohrs around each iron ion, is 3.6 for both complexes, which means that each iron ion is a high-spin d^6 Fe ion. The HOMO−LUMO gap for complex **1** and complex **2** is 0.48 and 0.31 eV, respectively.

(9) Pederson, M. R.; Khanna, S. N. *Phys. Rev. B* **1999**, *60*, 9566.

(10) (a) Kortus, J.; Pederson, M. R.; Baruah, T.; Bernstein, N.; Hellberg, C. S. *Polyhedron* **2003**, *22*, 1871 and references therein. (b) Ribas-Arino, J.; Baruah, T.; Pederson, M. R. *J. Chem. Phys.* **2005**, *123*, 044303. (c) Takeda, R.; Mitsuo, S.; Yamanaka, S.; Yamaguchi, K. *Polyhedron* **2005**, *24*, 2238.

(11) (a) Baruah, T.; Pederson, M. R. *Chem. Phys. Lett.* **2002**, *360*, 144. (b) Baruah, T.; Pederson, M. R. *Int. J. Quantum Chem.* **2003**, *93*, 324.

(12) (a) Hohenberg, P.; Kohn, W. *Phys. Rev.* **1964**, *136*, B864. (b) Kohn, W.; Sham, L. J. *Phys. Rev.* **1965**, *140*, A1133.

(13) (a) Pederson, M. R.; Jackson, K. A. *Phys. Rev. B* **1990**, *41*, 7453. (b) Jackson, K. A.; Pederson, M. R. *Phys. Rev. B* **1990**, *42*, 3276. (c) Porezag, D. V. Ph.D. Thesis, Chemnitz Technical Institute, 1997.

(14) Perdew, J. P.; Burke, K.; Ernzerhof, M. *Phys. Rev. Lett.* **1996**, *77*, 3865.

(15) Porezag, D.; Pederson, M. R. *Phys. Rev. A* **1999**, *60*, 2840.

Table 2. Fe^{II} Coordination Bond Lengths of the Optimized Structures of Both Complexes[a]

bond lengths	$[Fe_4(sap)_4(MeOH)_4]$	$[Fe_4(sae)_4(MeOH)_4]$
Fe−N	2.112	2.003
Fe−O(1)	2.007	1.972
Fe−O(2)	2.058	2.133
Fe−O(3)	2.182	2.111
Fe−O(4)	2.198	2.298
Fe−O(5)	2.257	2.226

[a] All the values are given in Å. In $[Fe_4(sap)_4(MeOH)_4]$, the four iron ions are symmetrically equivalent. In $[Fe_4(sae)_4(MeOH)_4]$, the four iron ions are not symmetrically equivalent, and therefore, the given values are the average bond lengths. See Figure 4 to see how the coordinating atoms are labeled.

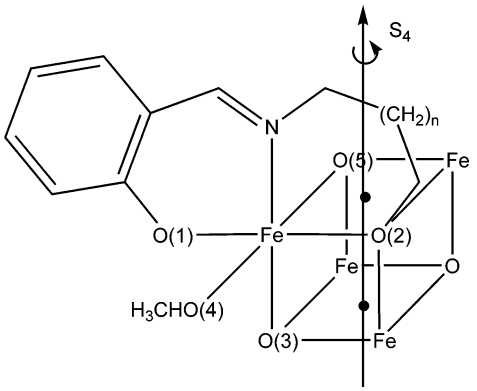

Figure 4. Schematic representation of complex **1** and complex **2**. Only one of the Fe^{II} coordination environments is depicted for clarity. The other ones are equivalent by symmetry. The *n* of $(CH_2)_n$ is equal to 1 for complex **1** and equal to 0 for complex **2**.

The calculations carried out on the magnetic anisotropy of complex **1** allow us to conclude that the system is an easy-plane system, with the easy plane being perpendicular to the S_4 axis of the complex (see Figure 4). The *D* value is 0.25 K and *E* is exactly 0 K because of the symmetry of the complex.

On the other hand, the calculations carried out on the magnetic anisotropy of complex **2** show that this system is an easy-axis system, with the easy axis being collinear to the *pseudo*-S_4 of the system (the symmetry of this complex is close to the S_4 one). The calculated anisotropy Hamiltonian parameters are $D = -0.10$ K and $E = 0.004$ K, which lead to an MAE barrier of 5.6 K.

Our results are in qualitative agreement with the experimental findings[8] because they correctly predict that complex **2** is an SMM, while complex **1** is an easy-plane system. The experimental *D* values for complex **1** and complex **2** are 1.15 K and −1.09/−0.44 K,[16] respectively. As can be seen, the calculated values are smaller than the measured ones. One of the reasons for this fact may be the absence of higher-order terms in our treatment of spin−orbit coupling. However, it should be mentioned that the experimental techniques used to obtain these values (dc and ac magnetic susceptibility measurements) usually provide less reliable values than those that can be determined from high-field EPR measurements. On the other hand, it is worth mentioning that, in these systems, the intramolecular exchange coupling constants are quite small[8] (on the range between 1.7 and 2.8 K, for the $\hat{H} = -\sum_{ij} J_{ij} S_i S_j$ Hamiltonian), which means that the $S = 7$ state must be close to the $S = 8$ ground state. The closeness of this excited state could have a non-negligible effect on the value of *D* and, consequently, on the MAE barrier. Our calculations are only dealing with the $S = 8$ ground state, and that could be another reason for not getting a quantitative agreement with the experimental data. The important point, though, is that we are able to reproduce the experimental trends. We will now turn our attention to the structural and electronic factors responsible for these trends, and with the information obtained with this analysis, we will be able to make a prediction on how to increase the MAE barrier of Fe^{II}-based SMMs.

Discussions

To rationalize the change of the sign of the *D* value in going from complex **1** to complex **2**, we have carried out calculations of the atom-projected anisotropies on each iron ion of both complexes. These calculations are usually useful because the *D* value of the complex is generally provided by a tensorial sum over constituent atoms.[17] The first issue concerning these calculations is that the Fe^{II} ions with their local coordination environment are triaxial or rhombic systems, possibly because their geometry is very distorted with respect to the octahedral one. Therefore, the discussion will not be made in terms of local *D* values but in terms of the directions of the local quantization (or magnetization) easy axes.

As can be seen in the left side of Figure 5, the local easy axis of each iron ion in complex **1** is approximately perpendicular to the S_4 axis of the complex. Specifically, it forms an angle of 73.5° with the S_4 axis, which means that the projection of the local easy axis onto the S_4 axis is 0.2830. As for complex **2**, the projection of the local easy axis of each iron ion onto the *pseudo*-S_4 axis is 0.5370; that is to say, the angle between the local easy axis and the *pseudo*-S_4 is 57.5° (these two last values are the average values of the four iron ions). The increase of the projection of the local easy axes onto the S_4 axis causes the change of sign and magnitude of the *D* value of the system in going from complex **1** to complex **2**.

To understand and visualize the last statement, it is useful to bear in mind the two limiting cases that can arise, with reference to the alignment of the local easy axes. If all the local easy axes were lying on the O(1)−Fe−O(2) axes (or the O(4)−Fe−O(5) axes; see Figures 5 and 6), they would define a plane perpendicular to the S_4 axis, and therefore, the whole molecule would be an easy-plane system, with a positive *D* value. On the contrary, if all the local easy axes were lying on the O(3)−Fe−N axes (see Figures 5 and 6), a perfect collinear alignment of local easy axes would arise, and the system would be an easy-axis system, with a negative *D* value. Thus, it is evident that the limit in the first case will be the perfect easy-plane system, with the most positive *D* value (for this kind of systems), and the limit of the second case will be the perfect easy axis system, with the most negative *D* value that can be achieved with these ligands. Since the projection of the local easy axes onto the S_4 axis is a way to quantify the direction of these axes, we can conclude that the situation found in complex **2** is closer to the second limiting case than the situation found in complex **1**, which is very close to the first limiting case. The analysis of

(16) These two different values have been obtained with two different experimental techniques. The first value has been obtained from dc magnetic susceptibility data, and the second has been obtained from ac magnetic susceptibility measurements.

(17) Bencini, A.; Gatteschi, D. *Electron Paramagnetic Resonance of Exchange Coupled Systems*; Springer: Berlin, Tokyo, 1990.

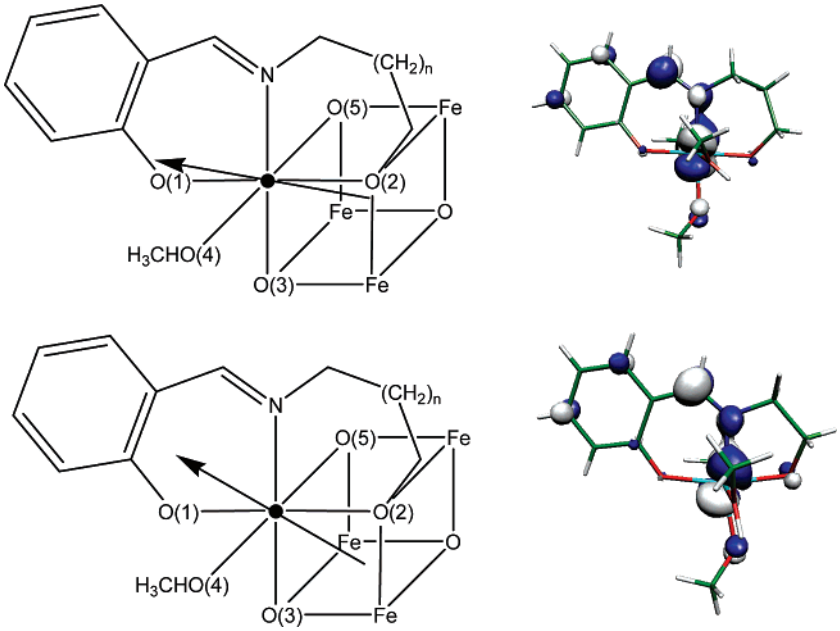

Figure 5. Direction of the local easy axis for complex **1** (up) and for complex **2** (down). Only one of the easy axes is depicted for clarity. On the right, the Fe^{II} d orbital which is doubly occupied for each of the iron ions constituting complex **1** (up) and complex **2** (down) is depicted. The *n* of $(CH_2)_n$ is equal to 1 for complex **1** and equal to 0 for complex **2**.

the projected anisotropies, thus, allows us to qualitatively justify why complex **2** is an SMM, whereas complex **1** is not an SMM.

After having discussed the different magnetic behaviors of complex **1** and complex **2** in terms of the atom-projected anisotropies, we will now focus our attention on the structural parameters responsible for such different behaviors. All the calculations carried out for determining the structural parameters that control the magnetic anisotropy in these systems have been performed with the model system depicted in Figure 7, in which the aliphatic $-(CH_2)_n-$ chain has been removed. In ref 8, it was argued, based on AOM (angular overlap model) calculations,[18] that the different magnetic behaviors of complex **1** and complex **2** could be attributed to the fact that, in complex **2**, the Fe^{II} ions have shorter coordination bond lengths at the equatorial positions (the Fe^{II} ions exhibit a Jahn−Teller distortion; the equatorial bonds are the shortest ones). Using the geometry of complex **1**, we have shortened all the equatorial bond lengths first by 0.02 Å and then by 0.04 Å and calculated the *D* value of the resulting complexes. These new *D* values remain practically unchanged with respect to the original value of 0.25 K. Consequently, we can conclude that the regular distortion associated with the shortening of the equatorial bond lengths of Fe^{II} ions is not the cause of the different magnetic behaviors of complex **1** and complex **2**. One of the reasons for the discrepancy between the DFT results and AOM results could be the fact that the AOM calculations have been carried out assuming a D_{4h} local coordination environment around the Fe^{II} ions.

Looking at the coordination bond lengths (see Table 2), one realizes that in complex **1**, the local easy axes lie approximately on the O(1)−Fe−O(2) axes, which are associated with the shortest bond lengths of the coordination environment of the Fe^{II} ions. As for complex **2**, the local easy axes lie between the O(1)−Fe−O(2) and the O(3)−Fe−N axes, i.e., between the Fe−O(1) and the Fe−N bonds, which are the shortest ones. Given these facts, one may think that in Fe^{II} coordination environments the local easy axes tend to be aligned with the shortest bond lengths. To test the validity of such a hypothesis, we have taken the geometry of complex **1** and we have lengthened the Fe−O(1) and Fe−O(2) bonds by 0.08 Å, and we have shortened the Fe−O(3) and Fe−N bonds by 0.08 Å, on the other hand. With these geometrical changes, the O(3)−Fe−N axes become the axes associated with the shortest bond lengths. The *D* value of the complex for the resulting geometry is 0.20 K. Such a small change with respect to the original value (0.25 K) clearly indicates that the former hypothesis is not valid. Variations of the bond lengths slightly more different than 0.08 Å (for instance, 0.02 Å, 0.04 Å, or 0.06 Å) lead to the same conclusion. The analysis of the atom-projected anisotropies confirm this result, since the direction of the local easy axes remain practically unchanged; i.e, they are almost aligned with the O(1)−Fe−O(2) axes.

The results shown so far seem to indicate that simple distortions regarding the coordination bond lengths do not have a dramatic effect on the Fe^{II} local anisotropies and, thus, in the magnetic anisotropy of the whole complex. Concerning the influence that the coordination bond lengths exert upon the magnetic anisotropy, the last calculation that has been carried out is the calculated *D* value of complex **1** with the coordination bond lengths of complex **2** (see Table 2). The calculated *D* value is 0.13 K. It can be seen that, in this case, the difference in coordination bond lengths (which cannot be described by a simple distortion) has a more important effect on the magnetic anisotropy than those for the previous cases. Nevertheless, it must be pointed out that only considering the bond distances is not enough to account for the change of sign of the *D* value in going from complex **1** to complex **2**. This is confirmed by the atom-projected anisotropies calculations, which show that the

(18) (a) Figgis, B. N.; Hitchman, M. A. *Ligand Field Theory and Its Applications*; Wiley-VCH: 2000. (b) Schönherr, T. *Top. Curr. Chem.* **1997**, *191*, 88. (c) Hoggard, P. E. *Coord. Chem. Rev.* **1986**, *70*, 85. (d) Lever, A. B. P. *Inorganic Electronic Spectroscopy*, 2nd ed.; Elsevier: 1984. (e) Larsen, E.; La Mar, G. N. *J. Chem. Educ.* **1974**, *51*, 633.

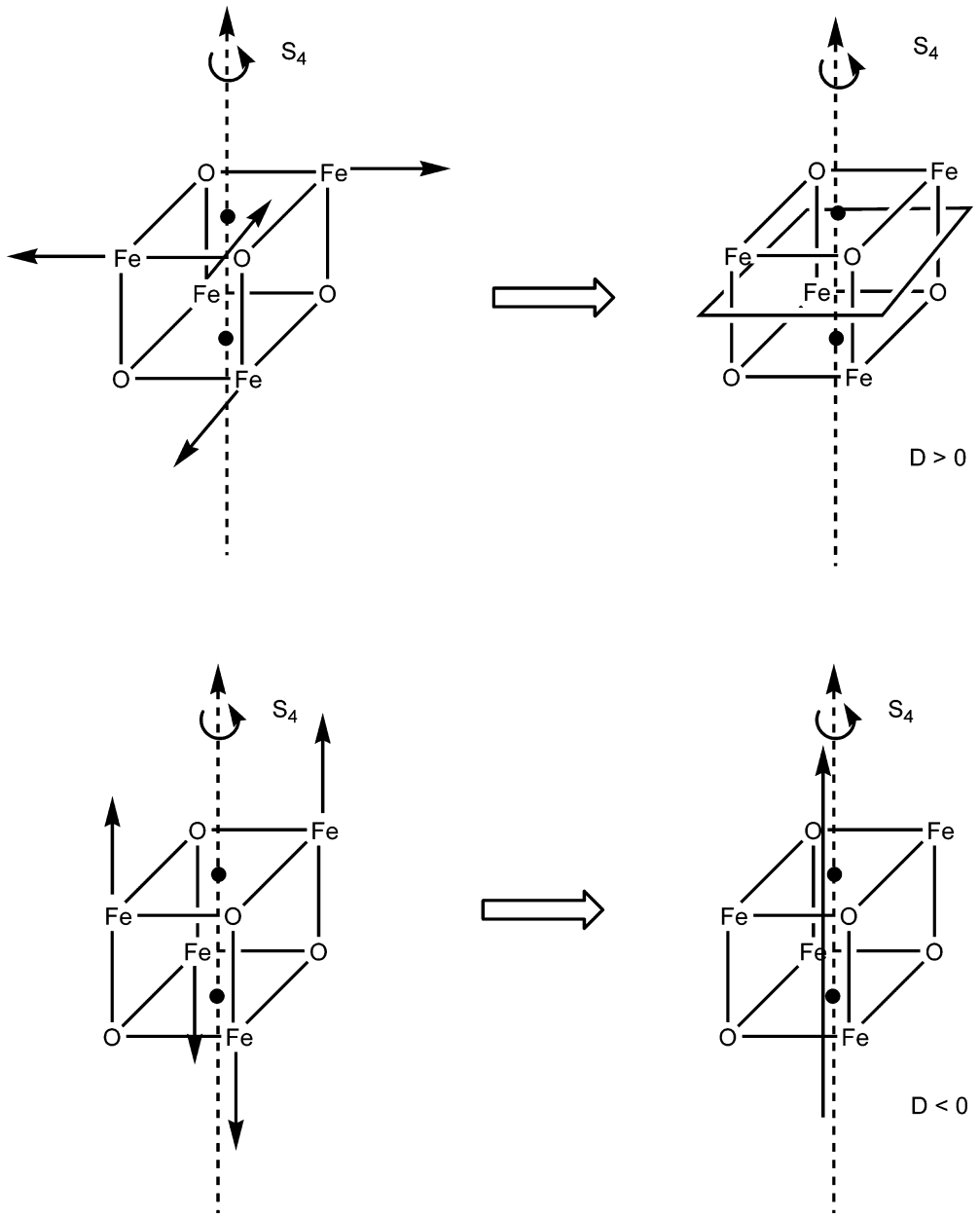

Figure 6. Orthogonal easy-axis alignment (up), which gives rise to an easy-plane system ($D > 0$), with the easy plane being perpendicular to the S_4 molecular axis. Collinear easy-axis alignment (down), which gives rise to an easy-axis system ($D < 0$), with the easy axis being collinear to the S_4 axis.

projection of the local easy axes onto the S_4 axis is 0.3515 (i.e., the angle between the local easy axes and the S_4 axis is 70°). This value lies between the value associated with the geometry of complex **1** (0.2830) and the value associated with the geometry of complex **2** (0.5370).

Apart from the differences in bond distances, the local coordination environments of Fe^{II} ions of complex **1** and complex **2** also differ for some bond angles. The most important structural difference with regard to the bond angles is found in the N−Fe−O(2) angle. This angle is 95.8° and 81.3° for complex **1** and complex **2**, respectively. This difference is due to the fact that the sap ligand (complex **1**) forms a six-membered chelate ring, whereas the sae ligand (complex **2**) forms a five-membered one with the Fe^{II} ions. If we take the geometry of complex **1** and change the N−Fe−O(2) angle to 81.3°, the resulting complex has a D value of 0.16 K. As with the bond distances, we can see that the difference in bond angles has a non-negligible effect on the magnetic anisotropy of the complex, although such a difference cannot account for the opposite magnetic behavior of complex **1** and complex **2** by itself.

As a conclusion of this structural study, we can say that the change of sign of the D value in going from complex **1** to complex **2** can be attributed not only to the change of coordination bond lengths but also to the change in bond angles, such as N−Fe−O(2), for instance. Therefore, there is not a single geometrical parameter responsible for the magnetic changes. In addition to this, all the results shown so far seem to indicate that it is very difficult to increase in a controlled way the magnetic anisotropy of these systems by only taking into consideration the geometrical distortions with the same kind of ligands. This is why we considered changing the electronic properties of the ligands in order to enhance such anisotropy.

Before considering the electronic properties of the ligands, it is interesting to point out that the results of our structural

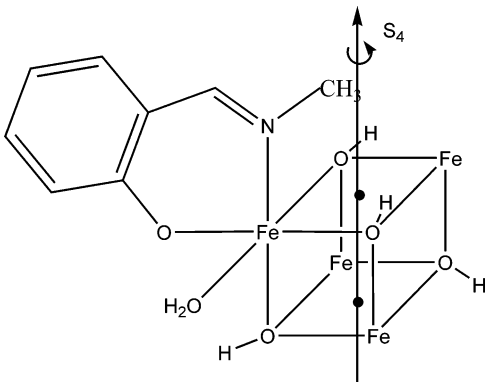

Figure 7. Model system used to determine the influence of structural factors on the magnetic anisotropy of complex **1** and complex **2**. Only the coordination environment of one iron ion is depicted for clarity. The other coordination environments are equivalent by symmetry.

analysis provide a quite different picture than the one provided by the AOM calculations performed in ref 8a. In ref 8a, the authors argued that the negative *D* value of complex **2** was due to a orthogonal alignment of the local hard axes of the four Fe^{II} ions (with positive local *D* values), whereas the positive *D* value of complex **1** was due to a orthogonal alignment of the local easy axes of the four Fe^{II} ions (with negative local *D* values). In both cases, the local hard axes or easy axes were assumed to lie on the O(4)−Fe−O(5) axes, i.e., the Jahn−Teller elongated axes. Our DFT calculations, on the contrary, show that the difference in magnetic behaviors between complex **1** and complex **2** has to be attributed to the different orientations of the local easy axes of the Fe^{II} ions of each complex. Moreover, the DFT calculations indicate that the local easy axes are not aligned with the Jahn−Teller elongated axes.

The molecular orbitals depicted in the right side of Figure 5 give us the first clue on how to change the ligands so as to have an SMM with an enhanced MAE barrier. The molecular orbitals depicted in Figure 5 are those associated to the doubly occupied Fe^{II} d orbital in all the Fe^{II} ions (d^6) of both complexes. Examining the direction of the local easy axes (see Figure 5) and the Fe^{II} d orbital, one may think about the following empirical rule: the local easy axis of each Fe^{II} ion points toward the perpendicular direction of the plane defined by the doubly occupied Fe^{II} d orbital. If this was true, one would *only* need to be concerned about the Fe^{II} d orbital which is doubly occupied in order to know the direction of the local easy axis. It is clear that such a simple rule would be extremely useful for the rational design of Fe^{II}-based SMMs. To test the validity of this hypothesis, we first need to know how to control the Fe^{II} d orbital which is doubly occupied for a high spin Fe^{II} in a given coordination environment. Once again, the molecular orbitals depicted in Figure 5 give us another clue. Looking at these orbitals, we realize that the direction of the Fe^{II} d doubly occupied orbital is mainly controlled by the π-back-donation of the Fe^{II} ion to the π antibonding orbitals of the imine fragment. Obviously, the other fragments of the sap or sae ligand can also exert an influence on the direction of the Fe^{II} d doubly occupied orbital, but it is logical to assume that the bonding combination of the Fe^{II} d orbital with the π antibonding orbitals of the imine fragment is the strongest interaction.

The calculation of the *D* value of the first compound of Figure 8 (this compound is obtained using the same geometry of $[Fe_4(sap)_4(MeOH)_4]$, but with the sap ligand replaced by the fragments shown in Figure 8) yields a value of 0.43 K. In this case, the *D* value is even more positive than that for the $[Fe_4(sap)_4(MeOH)_4]$ compound because the local easy axis of each Fe^{II} ion has a negligible projection onto the S_4 axis; i.e, this case is almost equivalent to the first limiting case we have referred to before (see Figure 5). This result supports the idea stated in the previous paragraph (see the direction of the local easy axis in Figure 8 and the Fe^{II} d doubly occupied orbital) and also shows that the projection of the local easy axis onto the S_4 axis is different depending on the presence or the absence of conjugation of the imine double bond with the aromatic ring of the sap ligand.

The most interesting result, however, is obtained for the second compound of Figure 8. This compound is the same of compound **1** in Figure 8, but the imine fragment and an hydroxyl ligand have had their positions switched. The *D* value of the resulting complex is −0.56 K, which means that switching the position of these two ligands yields a polynuclear complex that behaves as an SMM, with an MAE barrier of 36 K (this value is associated with the geometry of $[Fe_4(sae)_4(MeOH)_4]$; upon relaxation, the second compound of Figure 8 has an MAE barrier of 40 K). This is a remarkable result because the MAE barrier is increased by a factor of approximately 6 with respect to the barrier for the $[Fe_4(sae)_4(MeOH)_4]$ compound. This important increase of the MAE barrier is due to the orientation of the local easy axes of each iron ion. As can be seen in Figure 8, the local easy axes are almost collinear with the S_4 axis (their projection onto this S_4 axis is 0.9301), which makes this situation very similar to the second limiting case explained before (see Figure 5). The orientation of the local easy axes is, in turn, related to the plane defined by the Fe^{II} d doubly occupied orbital, since such local easy axes are, once again, perpendicular to this plane.

The definitive proof that our hypothesis concerning the direction of the local easy axes is valid is provided with the calculations of compound **3** of Figure 8. This compound is the same as compound **2** of Figure 8; the only difference is that, in compound **3**, the imine fragments have been rotated 90° with respect to the Fe−N axis. This means that the π orbitals of this fragment have also been rotated. As a consequence, each Fe^{II} d doubly occupied orbital is also rotated 90°, which results in a change of direction of the local easy axes. In this case, the local easy axes lie on the O(4)−Fe−O(5) axes. With this orientation, all the local easy axes are distributed in such a way that they define an easy plane (perpendicular to the S_4 axis). That is why the rotation of the imine fragment transforms compound **2** into an easy-plane system, with a *D* value of 0.49 K.

One may wonder whether these last results are specific for the imine double bond or whether they are more general and can be applied to other ligand systems with the proper orbitals so that the π-back-donation can take place. With this in mind, we have replaced the imine ligand of compound **2** (Figure 8) with the formaldehyde ligand and have calculated the *D* value for the resulting complex. This calculation yields a *D* value of −0.40 K (the associated MAE barrier is 26 K), with the local easy axes being collinear to the S_4 axis. Thus, this result seems to indicate that the π-back-donation-based strategy is quite general. Hence we may conclude that the control of the d orbital which is doubly occupied in a high-spin Fe^{II} by means of the π-back-donation allows one to control the direction of the

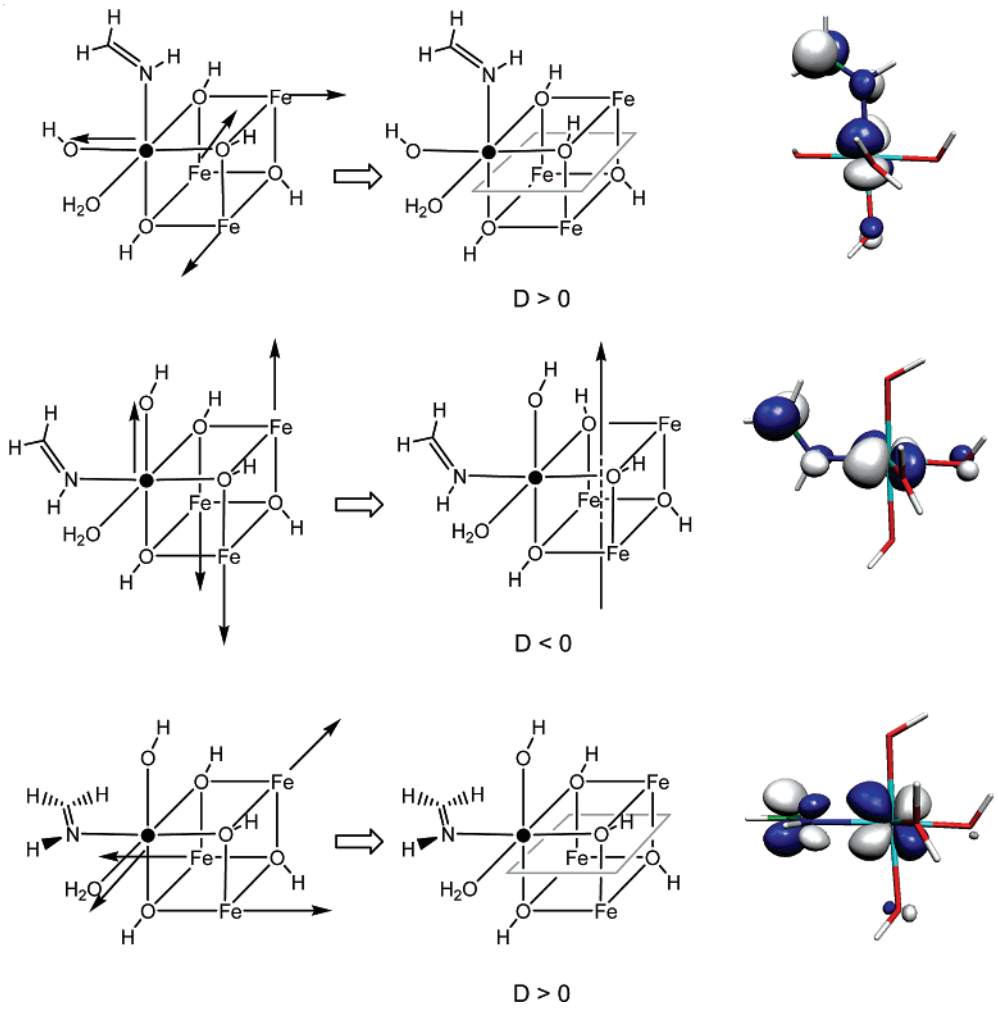

Figure 8. Small complexes (only the coordination environment of one iron is depicted for clarity) used to check the influence that the π-back-donation exerts on the magnetic anisotropy of Fe^{II} cube complexes. On the left, the local easy axis of each Fe^{II} can be seen. In the middle, the easy plane (for compound 1 and compound 3) or the overall easy axis (for compound 2) for each complex is depicted. On the right, it can be seen the Fe^{II} d orbital which is doubly occupied for all the Fe^{II} ions of the corresponding complex. As shown in this figure, the local easy axes are perpendicular to the plane defined by such an orbital.

corresponding local easy axis and, in turn, the anisotropy of the whole system.

It is well-known[19] that the magnetic anisotropy of polynuclear complexes depends on the local anisotropy of the individual magnetic building blocks and on their relative arrangements. It is also a well-established fact that the SMM behavior is achievable when the local easy axes of the magnetic building blocks are aligned or when the corresponding local easy planes are orthogonal. The problem is that the control of the local anisotropy of the magnetic building blocks is not obvious. Most of the SMMs reported so far are Mn^{III}-based polynuclear complexes.[4] This kind of SMMs has been analyzed considering that the local easy axes of the Mn^{III}-based magnetic building blocks are aligned with the corresponding Jahn−Teller elongated axes. Similar rules have not yet been established for other transition metal ions, though. Since such rules are essential in order to succeed in preparing new SMMs with enhanced properties, the theoretical studies concerning the local anisotropies of the magnetic building blocks are necessary and relevant.

The theoretical study we have presented provides synthetic chemists with a very simple rule to rationally prepare a new series of Fe^{II}-based SMMs. We have focused our study on cubane structures (such a study can also be extended to other kinds of structures), and our calculations on the small compounds of Figure 8 give some clues on how a proper ligand system has to be designed in order to have SMMs with a high MAE barrier. On the other hand, we have shown how the arguments based only on coordination bond lengths might not be enough in some cases when applied to rationalize the magnetic anisotropy behavior of polynuclear complexes. In relation to this, it seems that arguments based on molecular orbitals may be more general than geometrical arguments. This is the first time that DFT-based calculations of the magnetic anisotropy have established a very simple relation between the local anisotropies of metal ions and molecular orbitals. This suggests that if this kind of study is carried out for other metal ions, a set of simple rules for control of the magnetic anisotropy will be made available. These rules, together with the angular overlap model analyses,[20] would be very helpful for developing

(19) Gatteschi, D.; Sessoli, R. *Angew. Chem., Int. Ed.* **2003**, *42*, 268.

(20) (a) Gatteschi, D.; Sorace, L. *J. Solid State Chem.* **2001**, *159*, 253. (b) Boèa, R. Magnetic Parameters and Magnetic Functions in Mononuclear Complexes Beyond the Spin-Hamiltonian Formalism. *Structure and Bonding* **2006**, *117*, 1. (c) Oshio, H.; Nakano, M. *Chem.—Eur. J.* **2005**, *11*, 5178.

suitable strategies for the synthetic chemists to introduce the appropiate anisotropy in molecules.

Conclusion

We have carried out a density-functional study of the magnetic anisotropy of two Fe^{II}-based single molecule magnets. The calculated magnetic anisotropies are in qualitative agreement with the experimental data. The analysis of the atom-projected anisotropies have helped us to rationalize the different magnetic behaviors of both polynuclear complexes. We have also been able to predict how to significantly increase the magnetic anisotropy barrier of these compounds. This prediction has been made on the basis of a simple qualitative rule that takes into account the molecular orbitals. Further work should be done to see if it is possible to apply similar simple rules to other metal ions. This would make possible a complete rational design of technologically useful single-molecule magnets.

Acknowledgment. J.R acknowledges Universitat de Barcelona and "Ministerio de Educación y Ciencia" of Spain for the award of a Ph.D grant and for the award of another grant to perform a research stay in the U.S. Naval Research Laboratory. T.B. acknowledges the following NSF grants: HRD-0317607 and NIRT-0304122. M.R.P. was supported in part by ONR and the HPCMO. J.R. also thanks Prof. Juan J. Novoa, his Ph.D. advisor, for having given him the opportunity to work with T.B. and M.R.P.

JA061518R